

## Optimization and thermal analysis of radial ventilated brake disc to enhance the cooling performance

Rahim Jafari <sup>a,\*</sup>, Recep Akyüz <sup>b</sup>

<sup>a</sup> Department of Automotive Engineering, Atilim University, Ankara, Turkey

<sup>b</sup> R&D Center, Turkish Automotive Company (TOFAŞ), Bursa, Turkey



### ARTICLE INFO

**Keywords:**

Optimization  
Taguchi method  
Design of experiments  
Brake disc  
Thermal analysis

### ABSTRACT

Ventilated brake discs are preferable to automobile application because of their higher heat dissipation ability than solid discs. The shape, geometry and number of the cooling fins are interested parameters to be investigated to improve the cooling performance of the discs. In the present study, the optimum design of the brake disc with radial vanes is investigated numerically using the Taguchi design of experiments with taking into account nine design parameters. Finite element method is employed to simulate the detailed airflow and temperature distribution in the disc considering adjoined components as pads, rim, tire and dust shield. It has been found that the ventilation gap width has the highest impact on the brake disc cooling. The cooling time of the disc decreases 21% as the ventilation gap increases from 8 mm to 14 mm. In addition, it reduces about 10% with the increment of the channel width between two adjacent vanes (inverse of vane numbers from 43 to 30) and the twist point from 225 mm to 266 mm. In a decreasing order of importance, fin angle, inner and outer diameters of fin, dust shield, bell link and disc material affect the cooling performance of the ventilated disc.

### 1. Introduction

In the brake system of a vehicle, the frictional force between the brake disc and pads causes to decelerate or stop a vehicle when required. In this way, the kinetic and potential energies of the vehicle convert into the thermal energy. Due to the heat generation, the temperature of the brake components rises and the friction coefficient falls. In the cases of repeated braking or drag braking, dissipation of the thermal energy is essential to prevent the overheating of the components. The overheating of the disc and pads affects the components performance adversely and causes brake judder [1], thermal cracks and deformation of disc [2], premature wear and brake fluid vaporization [3]. Thermal performance of the solid brake discs has been extensively investigated including the numerical modeling of a single braking [4,5], repeated braking [6,7] and experimental analysis [8]. Based on the studies in the literature, the dominant cooling method in the brake disc-pads is convection [9]. Therefore, ventilated discs are currently employed in the vehicles to improve the convective cooling. A ventilated disc consists of two parallel rubbing surfaces connected by series of radial vanes or pins as shown in Fig. 1. It utilizes greater cooling area than solid disc. Besides, it treats as a centrifugal fan in which the surrounding cool air is drawn into the channels of the disc and passes through them to remove the generated heat.

\* Corresponding author.

E-mail address: [rahim.jafari@atilim.edu.tr](mailto:rahim.jafari@atilim.edu.tr) (R. Jafari).

## Nomenclature

$A$	Area, $\text{m}^2$
$C_p$	Specific heat, $\text{J}/(\text{Kg}\cdot\text{K})$
$C_{\epsilon 1}$	Constant, 1.44
$C_{\epsilon 2}$	Constant, 1.92
$h$	Heat transfer coefficient, $\text{W}/(\text{m}^2\cdot\text{K})$ , Joint conductance, $\text{W}/(\text{m}^2\cdot\text{K})$
$h_c$	Constriction conductance, $\text{W}/(\text{m}^2\cdot\text{K})$
$H_c$	Microhardness, Pa
$h_r$	Radiative conductance, $\text{W}/(\text{m}^2\cdot\text{K})$
$I$	Identity matrix
$k$	Thermal conductivity, $\text{W}/(\text{m}\cdot\text{K})$
$k$	Turbulent kinetic energy
$m$	Mass, Kg
$m_{asp}$	Surface roughness, asperities ratio
$n$	Normal vector
$n$	Number of responses
$p$	Pressure, Pa
$P$	Kinetic energy, J
$Q_f$	Frictional heat, W
$q$	Heat flux, $\text{W}/\text{m}^2$
$q''_f$	Frictional heat flux, $\text{W}/\text{m}^2$
$T$	Temperature, K
$u$	Velocity vector, m/s
$Y$	Response for the given factor level

### Greek symbols

$\mu$	Dynamic viscosity, $\text{Pa}\cdot\text{s}$
$\rho$	Coefficient of friction
$\rho$	Density, $\text{Kg}/\text{m}^3$
$\sigma$	Stefan's constant, $\text{W}/(\text{m}^2\cdot\text{K}^4)$
$\sigma_{asp}$	Surface roughness, asperities height, m
$\epsilon$	Turbulent dissipation rate, $\text{m}^2/\text{s}^3$
$\gamma$	Emissivity
$\gamma$	Heat partition factor

### Subscripts

$d$	Disc
$p$	Pad

Coulibaly et al. [10] numerically showed that the maximum temperature of the ventilated disc is about 47 °C lower than the solid disc with different surrounding air temperatures.

Qian [11] used computational fluid dynamics (CFD) and design of experiments (DOE) study to optimize the straight vane shape and numbers to achieve the maximum cooling performance. Due to the axial symmetric configuration of the disc, a sector of the disc containing a vane with periodical boundary conditions was studied. Three vane shape parameters were included and it was concluded that in a decreasing order of importance, the vane number, front edge radius, short-long vane length ratio and taper length improved the cooling performance. The optimization enhanced the cooling performance about 35%.

Voller et al. [12] performed CFD analysis for a disc with 30 straight vanes. The disc temperature of 100 °C and 600 °C as well as a range of disc rotational speeds of 40–450 rpm were included to obtain the convection, conduction and radiation heat transfers. It was concluded that at high speeds convection is predominant heat transfer mechanism with maximum of 57% total dissipated heat.

Jafari et al. [13] simulated the repetitive braking and considered all the braking components used in a common passenger vehicle including the rim, tire and dust shield. It was found that the heat transfer by the internal vanes of the disc was 58%–71% of the total convective heat transfer from the brake disc during the cooling step.

Palmer et al. [14] modeled 20° section of a pin vented brake disc. The disc consisting of three rows of 36 pins was implemented atmospheric temperature and pressure at the inlet and outlet boundaries in still air. Optimization of the first row profile and pin thickness were carried out and it was concluded that NACA0036 profile had the best heat transfer characteristics. Furthermore, 10% decrease in the thickness of the first row pin enhanced the heat transfer 6%. They [15] also identified that the optimized value of the ratio of the total wetted area within the disc to the total frontal area presented to the flow by the pins maximized the heat transfer rate.

Hwang et al. [16] investigated temperature variation of a straight vented disc during repeated braking. The simulated domain is symmetric section about the central plane. The non-uniform pressure and temperature distributions in the contact zone have been predicted.

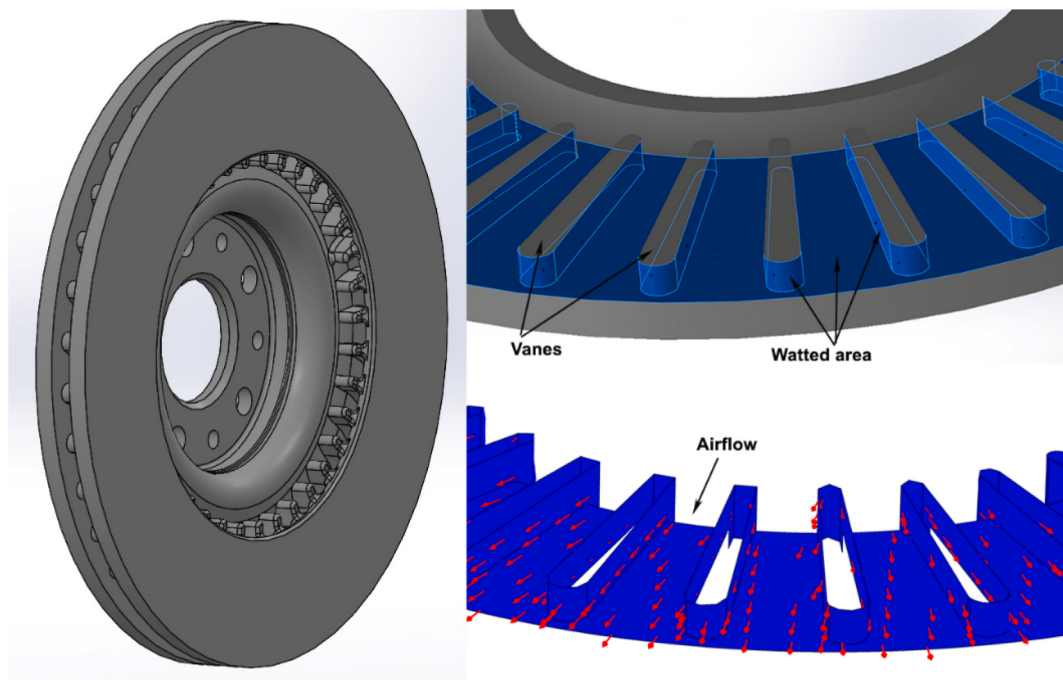


**Fig. 1.** Ventilated brake disc with split part showing wated area (blue color) and airflow passes through the vanes. (For interpretation of the references to color in this figure legend, the reader is referred to the Web version of this article.)

Stojanovic et al. [17] investigated the effect of the pressure in the contact zone on the temperature during the single braking. It was found that the maximum temperatures on the contact surface were 159.95 °C, 175.3 °C and 190.62 °C for the applied pressures of 0.9 MPa, 1 MPa and 1.1 MPa, respectively.

Galindo-Lopez and Tirovic [18] simulated a 24° segment of a ventilated brake containing two vanes. Periodic boundary conditions on the segmented sides were imposed. An additional small vane was installed in a channel between two main vanes to avoid air stagnation and recirculation. The results showed that the vanes placed at the channel outlets improved the heat transfer coefficient 6.7%. However, an inner position of the small vanes had detrimental effect on the heat transfer.

Pevec et al. [19] modeled a section of a brake disc containing three straight vanes. The applied periodic boundary conditions to the section sides consisted of ten cycles, each including one braking and one cooling from 100 km/h to zero and vice versa.

Modanloo and Talaee [20] analytically modeled thermal behavior of the brake discs in high speeds. A forced convection was applied on the inner surface to simulate the ventilation. The temperature gradient in disc thickness direction in ventilated disc was measured higher than the solid one. Moreover, the maximum temperature in the ventilated brake disc reduced to 659 °C compared to 782 °C for solid disc.

Yan et al. [21] introduced new heat dissipation medium instead of ventilated vanes and pins. Wire-woven bulk diamond material was highly porous and lightweight but mechanically strong. Not only did it reduce the disc temperature 16–36% compared to the pin-finned disc, but also led to more uniform heat transfer.

Kumar et al. [22] simulated the temperature distribution of three geometries of solid disc including drilled disc and drilled and slotted disc. The results revealed that the drilled and slotted disc had very high heat fluxes and lower temperature compared to the other discs.

Afzal and Mujeebu [23] modeled thermal performance of brake discs with different configurations under uniform convective heat transfer coefficients. It was resulted that the thermal performance of the disc improves by replacing the straight vents with curved ones. It further betters with making cross-drilled holes and slots.

Yan et al. [24] studied the effect of the cross-drilled holes on the ventilated brake disc. The simulation results for a segment of the disc revealed that cross-drilled holes enhanced the overall cooling 22–27%. The temperature of the cross-drilled disc was 141 °C less than that without cross-drilled ventilated disc for the extended downhill test with 400 rpm after 1 h. It also improved the cooling capacity of the pin-finned disc 15–17% [25].

Vdovin et al. [26] simulated the aerodynamics of a full vehicle to obtain the convective heat transfer. Afterward, the results were added to a thermal code to compute the conduction and radiation heat transfer. The results were subsequently utilized to recalculate the convection. The convection from internal vanes of the disc is 53% of the total convection of the disc at the end of the downhill test.

Qiu et al. [27] investigated the heat partition ratio between the brake disc and pads. Two-dimensional simulations revealed that in addition to material thermal properties and the contact area ratio, the thermal contact conductance affects the heat partition ratio. For high thermal contact conductance, the heat partition ratio to the brake disc is 95%.



**Fig. 2.** (a) Brake disc assembly, (b) Brake disc and its adjoins components.

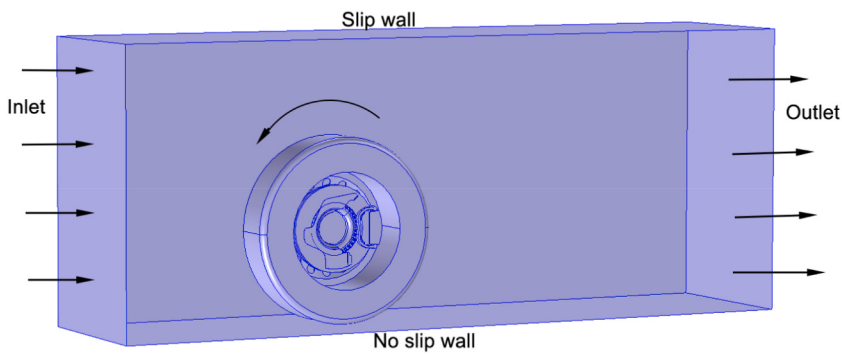


**Fig. 3.** Computational domain and boundary conditions.

Jian et al. [28] embedded bent heat pipes with a certain angle along the rotation direction on the outer surfaces of the brake disc. The experimental results represented that the heat dissipation increased by 12.62% and 18.90% respectively, during fifteen repeated and downhill braking methods. In addition, it enhanced the temperature uniformity in radial direction 36.67% and 21.43%, respectively for two of braking methods.

Hong et al. [29] used circular friction blocks on the brake pad to minimize the temperature and thermal stresses on the brake disc. The Taguchi design method along with the response surface method were employed to optimize the rate of friction heating. The maximum temperature, temperature gradient and the thermal stress of the disc reduced 16.8%, 55.2% and 11.2%, respectively by using optimized pad.

Yan et al. [30] reported that for the fixed inlet angle of 45° and rotational speed of 200–1000 rpm, increasing outlet angle from 45° to 135° improved the cooling performance of the disc up to 16%. Available studies in the literature have stressed that the radial vane brake discs generally have better cooling performance than the other types. However, very little studies have investigated their performance in the real boundary conditions. Moreover, it has not been reported a comprehensive work on the optimization of the geometry of the disc.

The aim of the current study is to optimize the geometry of the ventilated brake disc to maximize its cooling performance. Firstly, a three-dimensional model is designed to simulate the aerodynamics and thermal behavior of the ventilated brake disc. The model contains the ventilated brake disc and the adjoined parts including the pads, tire, rim, dust shield and caliper. Then the design of experiments is used to evaluate the effect of the each adjustable parameter on the cooling performance of the disc.

In section 2, the numerical model to simulate the ventilate brake disc and the optimization method are explained. Section 3 represents the numerical and optimization results. Section 4 concludes the achievements of the research.

## 2. Material and method

This section contains two subsections. Firstly, the numerical model for the simulation of the brake disc is described. Next, the optimization method of the cooling performance is explained.

### 2.1. Numerical model

#### 2.1.1. Computational domain

The brake disc, pads and the adjacent parts are shown in Fig. 2. Some of the components as knuckle, bearing and unnecessary

**Table 1**  
Initial and boundary conditions of the domain.

Parameter	Value
Inlet velocity	28.6 m/s
Outlet pressure	1 atm
Side walls and upper wall condition	slip
Lower wall condition	No slip
Initial temperature of the domain	25 °C
Initial temperature of the disc and pads	400 °C

**Table 2**  
Design parameters and the interval levels.

No	Control Factor	Visual	Levels			
1	Disc material		GLH160	GLL190		
2	Bell link		out	in		
3	Ventilation gap (mm)		8	10	12	14
4	Fin numbers		30	36	43	50
5	Fin inlet radius (mm)		5	8		
6	Fin outlet radius (mm)		9	12		
7	Fin angle (°)		0	22.5	37	45
8	Twist point of fin (mm)		225	266		
9	Dust shield		Full	Reduced		

details as fasteners, treads and holes are removed to reduce the computational time and energy. Fig. 3 represents the computational domain and boundary conditions. The airflow enters the domain from the inlet, passes through the channel, and leaves it from the outlet. The rotational motion of the tire, rim, disc and hub is proportional to the speed of the car. Slip wall boundary condition is assigned to the side walls and upper wall to reduce their effect on the airflow. The initial and boundary conditions are given in Table 1.

### 2.1.2. Aerodynamic-thermal model

The simulation contains two steps. Firstly, k- $\epsilon$  turbulent model is employed to calculate the velocity and pressure distributions. The steady-state simulation is conducted to obtain the velocity and pressure distributions as well as to save the computational time and energy. Next, the obtained velocity and pressure distributions are used to compute the convective heat fluxes and the temperature distribution transiently by the energy equation.

The well-known Navier-Stokes equations for k- $\epsilon$  turbulent model are solved to describe the velocity and pressure fields for the computational domain as

$$\rho \nabla \cdot (\mathbf{u}) = 0 \quad (1)$$

$$\rho (\mathbf{u} \cdot \nabla) \mathbf{u} = \nabla \cdot [-p\mathbf{I} + (\mu + \mu_T)(\nabla \mathbf{u} + (\nabla \mathbf{u})^T)] \quad (2)$$

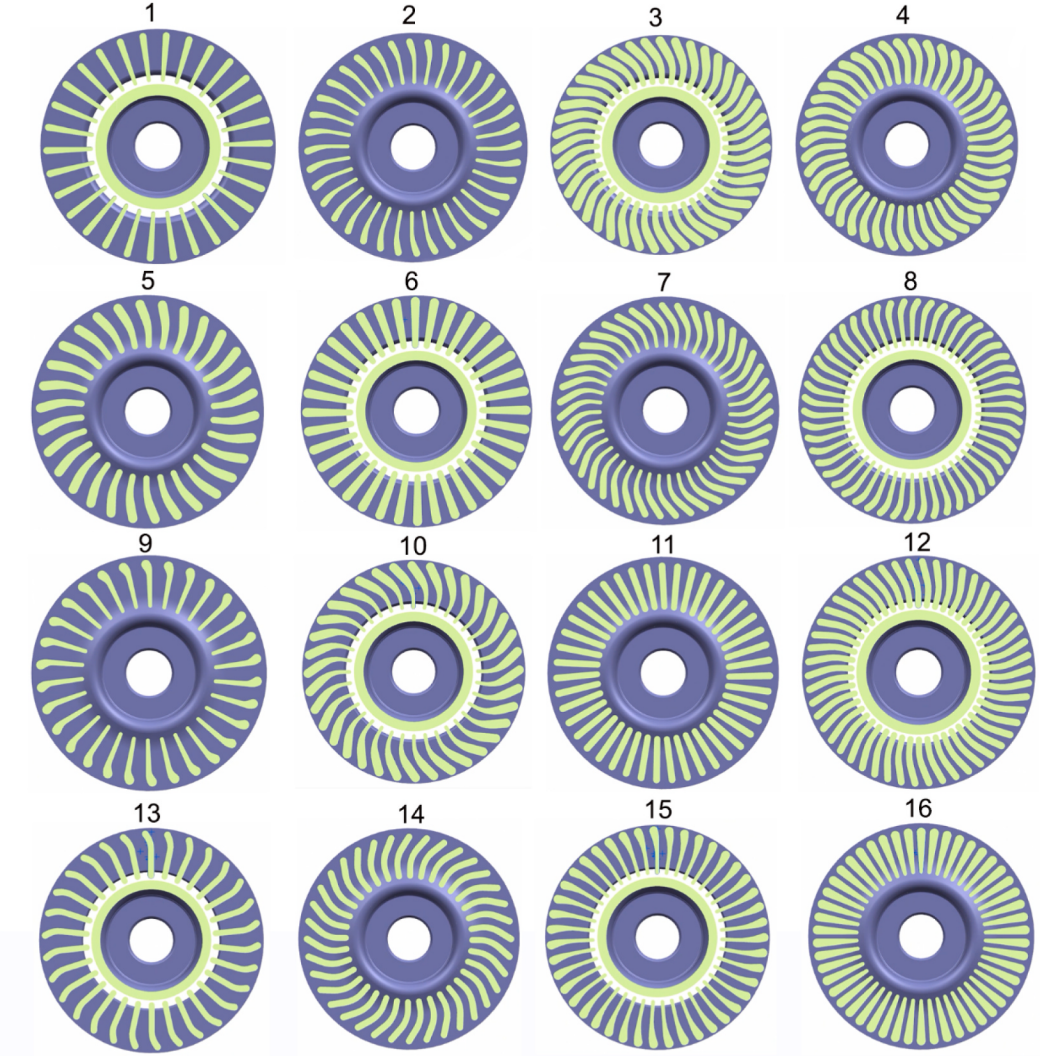


**Fig. 4.** Cross sectional view of the Taguchi L16 design for radial ventilated brake disc.

$$\rho(\mathbf{u} \cdot \nabla)k = \nabla \cdot \left[ \left( \mu + \frac{\mu_T}{\sigma_k} \right) \nabla k \right] + \mu_T [\nabla \mathbf{u} : (\nabla \mathbf{u} + (\nabla \mathbf{u})^T)] - \rho \varepsilon \quad (3)$$

$$\rho(\mathbf{u} \cdot \nabla)\varepsilon = \nabla \cdot \left[ \left( \mu + \frac{\mu_T}{\sigma_\varepsilon} \right) \nabla \varepsilon \right] + C_{\varepsilon 1} \frac{\varepsilon}{k} \mu_T [\nabla \mathbf{u} : (\nabla \mathbf{u} + (\nabla \mathbf{u})^T)] - C_{\varepsilon 2} \rho \frac{\varepsilon^2}{k} \quad (4)$$

The energy equation is used to simulate the temperature distribution for 3D Cartesian coordinate as

$$\rho C_p \frac{\partial T}{\partial t} + \rho C_p \mathbf{u} \cdot \nabla T - \nabla \cdot (k \nabla T) = Q \quad (5)$$

## 2.2. Optimization procedure

Nine design parameters of the brake disc were considered to be investigated. Taguchi method was used for the design of experiments (DOE). This method uses a special design for orthogonal arrays that makes it possible to study the whole parameter space using a limited number of experiments [31]. Table 2 represents the design parameters and the intervals between the assigned levels. The ranges of the design parameters were selected due to the manufacturing and economic restrictions. Two common material types, low carbon and high carbon gray cast irons are considered for the brake disc. It is possible to connect the disc to the flange in two ways. The flange or top hat would be connected to the inner or outer friction rings. The ventilation gap is another parameter that 8–14 mm is assigned at 2 mm intervals. Furthermore, the inlet diameter and the outlet diameter of the vanes as well as their angle and numbers are evaluated. The last investigated parameter is dust shield, which would cover the disc on inlet side in two shapes of full and reduced.



**Fig. 5.** (a) Experimental test setup, (b) positions of the embedded thermocouples.

**Table 3**  
Grid sizes with corresponding computational times.

Grid size	Grid numbers	Computational time
coarser	683445	6h 21min
coarse	1226900	20h 57min
normal	2457090	43h 24min
fine	3226632	91h 11min

The time required to dissipate the generated braking heat in the brake disc from 400 °C to 100 °C is the objective function and is desired to be minimum.

Taguchi L16 design with mixed 2–4 levels is used to evaluate the effect of the aforementioned design parameters on the brake disc temperature. Fig. 4 illustrates the section view of the sixteen designed discs.

The main effect analysis for the signal to noise (S/N) ratio is carried out to determine the effect of each design parameter on the objective function. The S/N ratio measures how the response varies relative to the target value under different noise conditions. As the highest and lowest S/N ratios variation is large, the effect of the parameter on the response is high. In order to minimize the dissipation time of the generated heat by the braking from 400 °C to 100 °C, the S/N formula for “smaller is better” is used in this analysis as

$$S/N = -10\log \left( \sum (Y^2)/n \right) \quad (16)$$

### 2.3. Validation of the numerical model

The numerical model is validated against the experimental result. Fig. 5 shows the test setup and the temperature measurement location inside the disc. The experiment is performed by the brake dynamometer available in FIAT as shown in Fig. 5a. The J type thermocouple with temperature accuracy of ±3.3 °C is embedded in the disc, 3 mm below the rubbing surface as illustrated schematically in Fig. 5b.

The ventilated brake disc is preheated up to 400 °C through the repetitive braking and then is cooled by constant speed of 105 km/h. Airflow with speed of about 35 km/h and temperature of 25 °C blows through a channel in the brake disc.

In addition, the simulations are performed with four different grid sizes as are given in Table 3. Those are carried out just as the same boundary conditions in the experiment to compare the results. Fig. 6 compares the experimental result and numerical results of four different grid sizes for the disc cooling from 400 °C. Although the relative error of cooling rate between the simulations with fine and normal grids is less than 5%, the computational time with the fine grids is more than twice of the normal grids. It is worth mentioning that for sixteen design of Taguchi L16, it takes extra one month to perform the simulations with fine grids rather than the normal grids. There is a very good agreement in the cooling rate of the brake disc between the simulation with normal grids and experimental result, with a maximum deviation of 12.5%. Therefore, the simulations of the optimization design are accomplished with

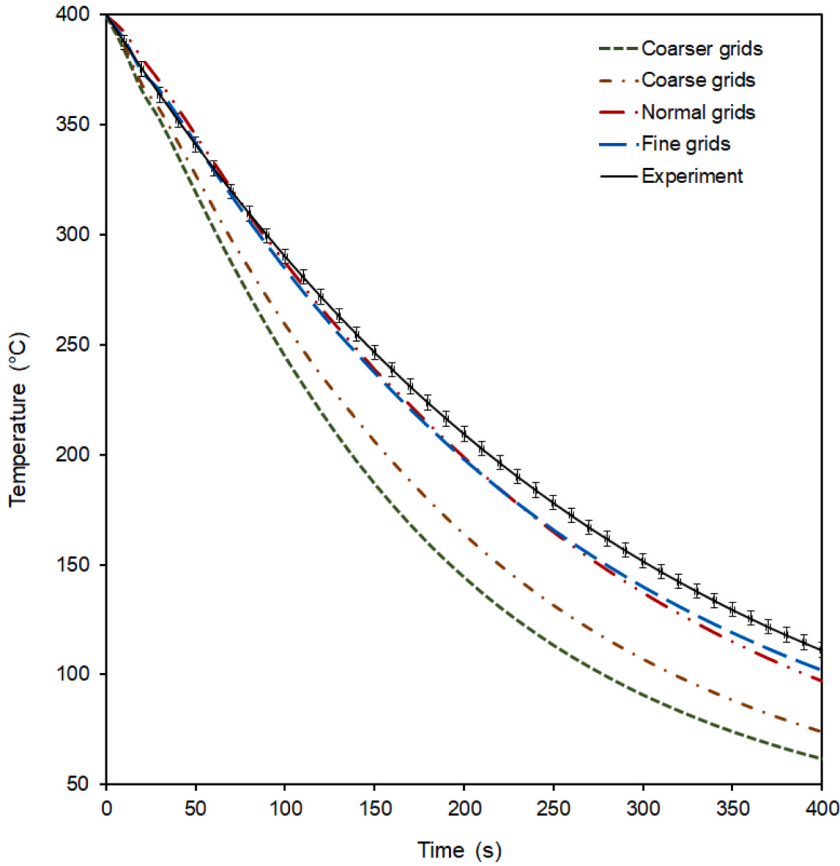


Fig. 6. Comparison of the simulation results with various grid sizes and the experimental result.

the normal grid size. Fig. 7 illustrates the mesh distributions for the disc and pads (Fig. 7a) and the section view of the radial vanes of #13 (Fig. 7b) and #16 (Fig. 7c). Tetrahedron grids are used in the geometry whereas the prism ones are employed in the boundary layers.

### 3. Results and discussion

In this section, firstly the aerodynamics and thermal behavior of the brake disc are investigated. Next, the optimization method and the effect of the variation of the design parameters on the ventilated brake disc are described and discussed.

#### 3.1. Fluid flow and thermal behaviors

The simulation demonstrates the detailed movement of the airflow around the brake components. Fig. 8 displays the velocity distribution and streamlines in the computational domain. The airflow contacts with the front of the tire and the velocity drops to near zero. It slides on the tire, which its value increases. Because of the relative velocity between the rotating wheel and the airflow, the velocity values on the corners of tire rise over the mainstream velocity. The velocity of airflow at the mainstream, 105 km/h, drops to less than 40 km/h over the brake disc as shown in Fig. 8a.

Although the velocity inside the rim is lower than the mainstream, a turbulent flow is captured inside the rim as shown in Fig. 8b. There is a complex turbulent flow inside the rim due to the simultaneous translational and rotational motions of the wheel.

Fig. 9 demonstrates a cross sectional view of the streamlines at the inner surface of the ventilated gap. It captured some eddies of swirling airflow with different intensities as shown in Fig. 9a. The direction of the airflow at the channels from the inlet to the outlet between the vanes is clearly visible by the streamlines as shown in Fig. 9b. The disc rotates in the counterclockwise direction. Considering the rotation direction, two distinctive regions are established for the flow in the channels. At the first region, adjacent to the leading side of the trailing vanes, the airflow speed is much higher than that at the leading side of the channels. These separated flow regions in the channels have been also detected experimentally using particle image velocimetry (PIV) method [32].

Fig. 10 shows the temperature distribution at three parallel surfaces of the disc during the braking. The generated frictional heat in the contact region causes hot spot appearance on the contact surface of the disc. The maximum temperature on the disc occurs on the contact region between the disc and the pad and it rises up to about 400 °C. The predominant heat transfer is convection during the disc rotation. Because of the radial vanes, the convection on the inner surface of the disc is more effective than that on the rubbing surface.

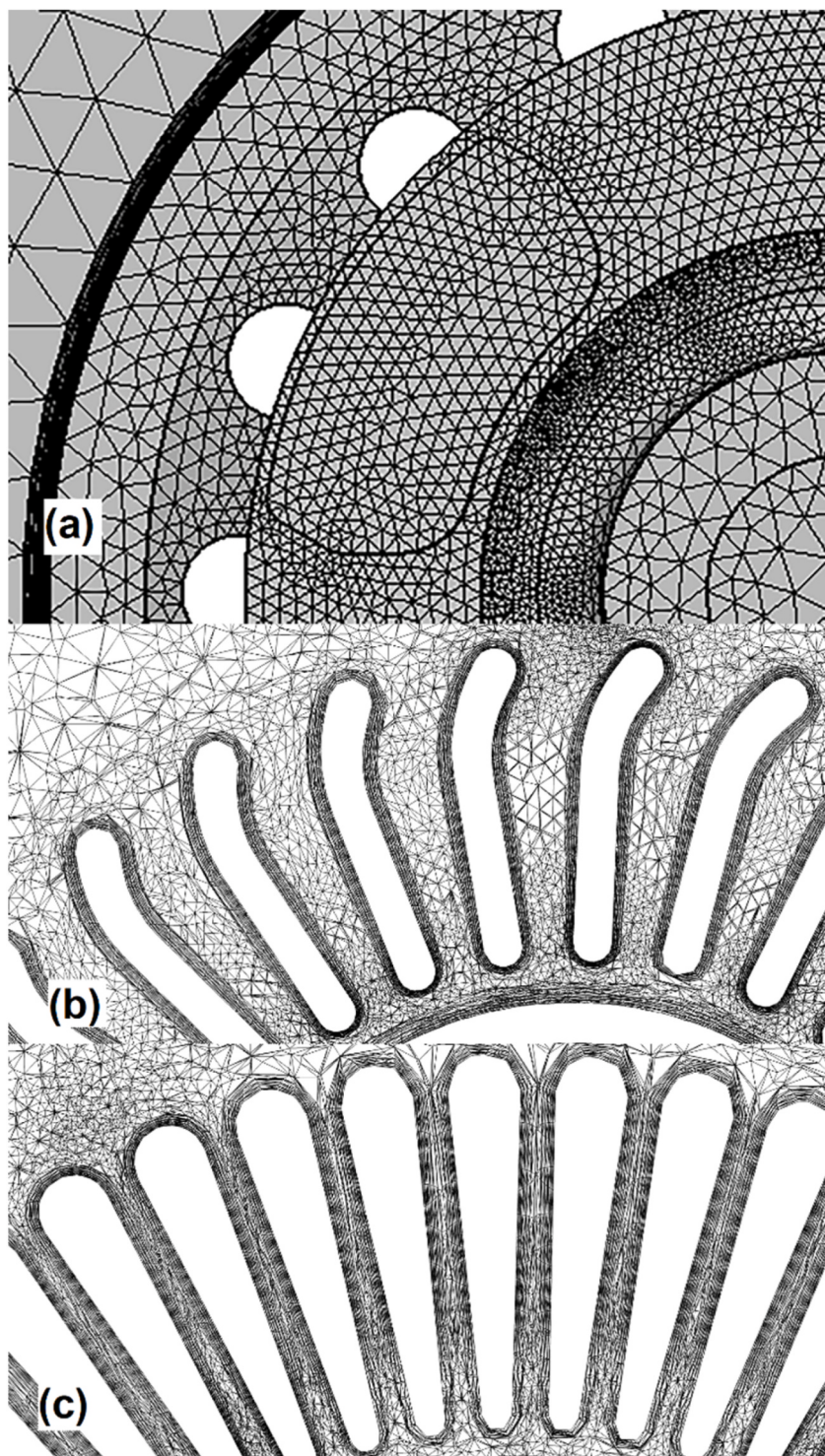


**Fig. 7.** Grids distribution for (a) the disc and the pad, (b) section view of the radial vanes of #13 design and (c) section view of the radial vanes of #16 design.

The temperature of the inner surface is about 80 °C less than that of the contact surface. Therefore, a temperature gradient appears in axial direction from the contact surface to the inner surface.

To quantify the effect of the cooling vanes, the temperature is predicted on the line in which passes through the measured points as shown in Fig. 5-b along the disc width. Fig. 11 displays the temperature distribution on the line along the disc width in the period of 0.6 s while the rotational speed is 105 km/h. When there is no contact between the disc and pads, the temperature distribution is

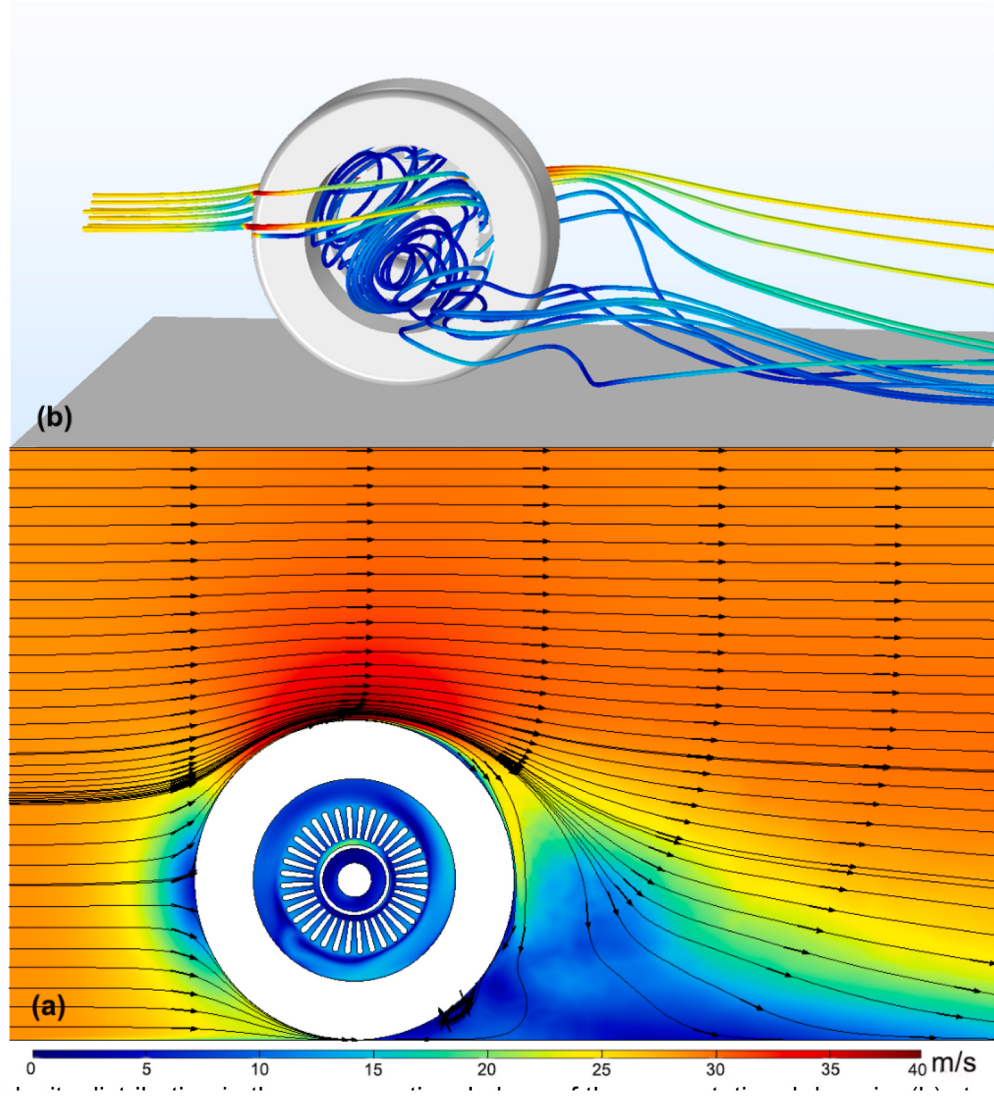


**Fig. 8.** (a) Velocity distribution in the cross sectional plane of the computational domain, (b) streamlines in and around the wheel.

approximately uniform and is predicted about 340 °C. Although the temperature of the rubbing surfaces increases locally and reaches to near 410 °C as the disc contacts the pads, the temperature of the vanes remains approximately constant. There is a slight difference in the temperature distribution of the two sides of the disc because of the asymmetric boundary conditions.

### 3.2. Optimization of the brake disc

Sixteen simulations are performed based on the Taguchi design with nine design parameters and 2–4 mixed discrete levels. Cooling time for each design, which is required to drop the temperature from 400 °C to 100 °C on the same point of the brake disc are given in [Table 4](#).

The analysis was conducted for each response parameter to investigate the change of the design parameters effect on the response. Main effects of design parameters for S/N ratios and means are given in [Fig. 12](#). It can be specified from [Fig. 12](#) that the ventilation gap has the strongest effect on the brake disc cooling. The cooling time of the disc decreases 21% as the ventilation gap increases from 8 mm to 14 mm. The increase of twist point, the channel width between two adjacent vanes (inverse of fins amount) and the fin angle have also considerable improvement on the thermal performance. Increase in the diameter of the twist point of the vanes from 225 mm to 266 mm and reduction in the numbers of the vanes from 50 to 30 reduce the cooling time about 10%. In addition, rising the angle of the vanes from zero to 37° enhanced the cooling near 7%. However, the inner and outer diameters of vanes and the dust shield show a slight effect (4%) on the heat dissipation. The effect of the bell link and disc material are negligible.

A linear regression to predict the cooling time from 400 °C to 100 °C is defined as

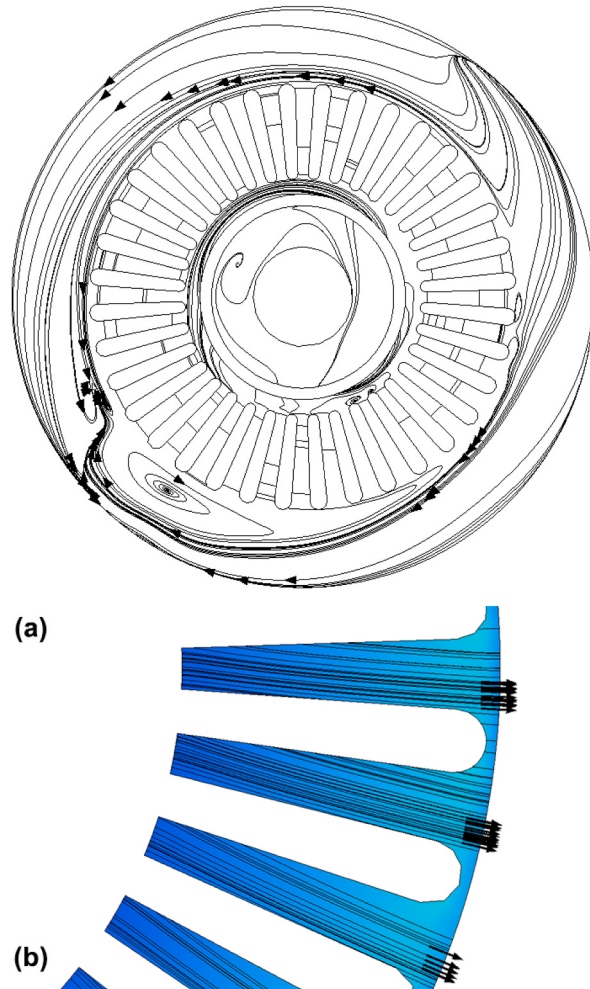


**Fig. 9.** Streamlines distribution (a) in and around the disc, (b) in the channels between the vanes.

$$t_{cooling} = 751 - 13.45 \text{ ventilation gap} + 0.69 \text{ fin amount} + 0.146 \text{ fin angle} + 5.91 \text{ fin inner diameter} + 6.00 \text{ fin outer diameter} - 1.171 \text{ twist point} - 9.3 \text{ bell link} + 18.3 \text{ dust shield} - 12.7 \text{ material} \quad (17)$$

where numbers 1 and 2 are assigned for first and second levels of bell link, dust shield and material, respectively.

According to the S/N ratio results and the correlation above, the best cooling time and the corresponding parameter levels are given in [Table 5](#). The optimized cooling time from 400 °C to 100 °C is predicted 334 s for ventilated brake disc.

#### 4. Conclusion

A comprehensive investigation into the overall cooling performance of the ventilated brake disc was carried out. Initially, the three-dimensional numerical model provided the detailed airflow and temperature distributions in the ventilated brake disc. The model contained the ventilated brake disc and the adjoined parts including the pads, tire, rim, dust shield and caliper. Moreover, Taguchi L16 design and S/N ratios and means were used to evaluate the effects of nine parameters on the cooling performance of the disc from 400 °C to 100 °C. According to the analysis results, the following findings were concluded:

- The ventilation gap width was the most effective parameter in the cooling of the brake disc. The amount of the airflow and the cooling area were increased by increasing the gap from 8 mm to 14 mm, which eventually enhanced the heat transfer from the disc.
- Increase in the diameter of the twist point of the vanes from 225 mm to 266 mm, reduction in the numbers of the vanes from 50 to 30 and rising the angle of the vanes from zero to 37° enhanced the heat transfer considerably.
- The reduction in the inner diameter of vanes from 8 mm to 5 mm and the outer diameter of vanes from 12 mm to 9 mm, besides using the reduced dust shield, enhanced the cooling of the disc slightly.
- The effects of the bell link as well as the low carbon and high carbon materials of the disc were negligible.

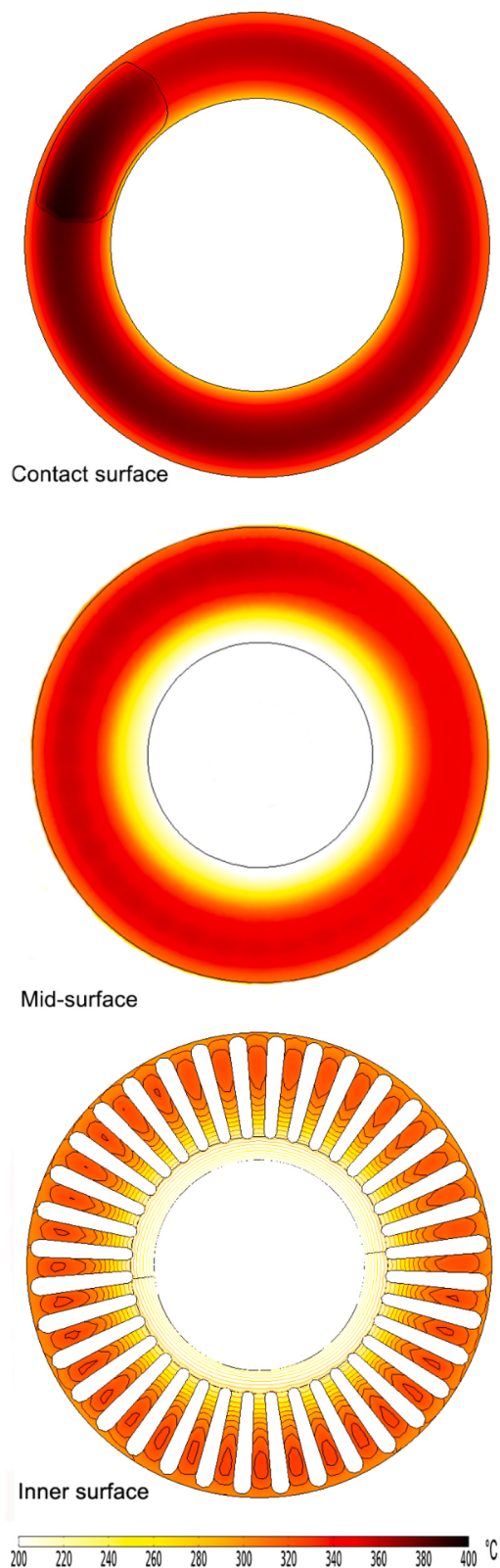


Fig. 10. Temperature distribution at three parallel surfaces of the disc during the braking.

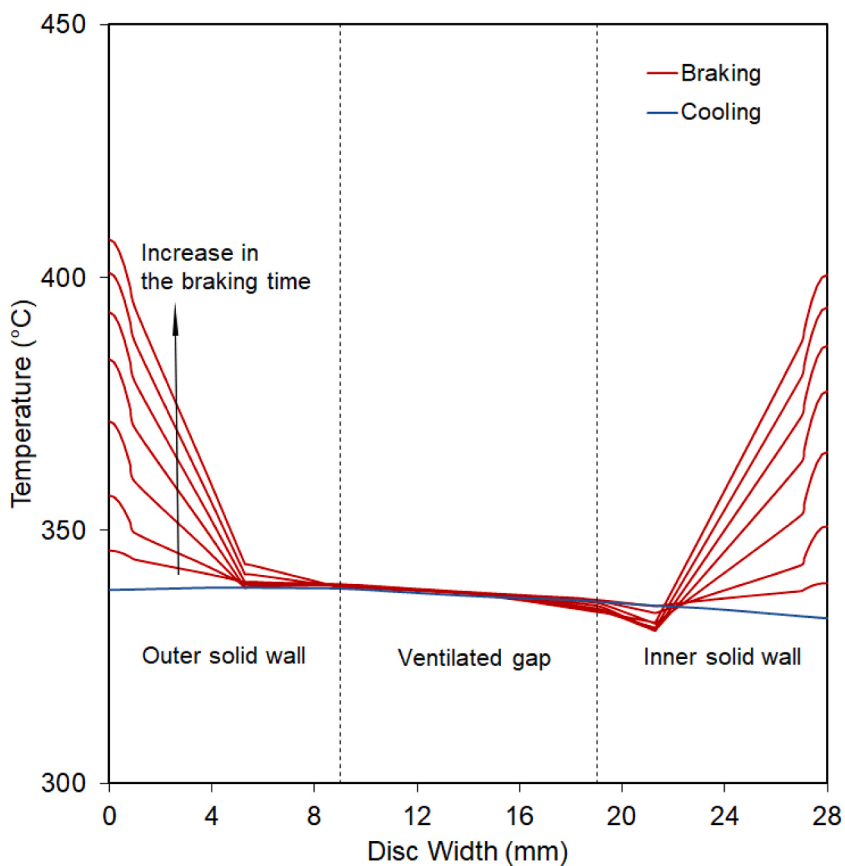


Fig. 11. Temperature distribution on the line along the disc width in the period of 0.6 s.

**Table 4**  
Taguchi L16 design for the ventilated brake disc and the cooling time results.

NO	Ventilation Gap (mm)	Fin Amount	Fin Angle (°)	Fin Inner diameter (mm)	Fin Outer diameter (mm)	Twist Point	Bell Link	Dust Shield	Material	Cooling Time from 400 °C to 100 °C (s)
1	8	30	0	5	9	225	In	Reduced	GLH160	486
2	8	36	22.5	5	9	266	Out	Full	GLL190	465
3	8	43	37	8	12	225	In	Full	GLL190	574
4	8	50	45	8	12	266	Out	Reduced	GLH160	497
5	10	30	22.5	8	12	225	Out	Reduced	GLL190	430
6	10	36	0	8	12	266	In	Full	GLH160	395
7	10	43	45	5	9	225	Out	Full	GLH160	455
8	10	50	37	5	9	266	In	Reduced	GLL190	344
9	12	30	37	5	12	266	Out	Full	GLH160	410
10	12	36	45	5	12	225	In	Reduced	GLL190	460
11	12	43	0	8	9	266	Out	Reduced	GLL190	429
12	12	50	22.5	8	9	225	In	Full	GLH160	520
13	14	30	45	8	9	266	In	Full	GLL190	370
14	14	36	37	8	9	225	Out	Reduced	GLH160	383
15	14	43	22.5	5	12	266	In	Reduced	GLH160	422
16	14	50	0	5	12	225	Out	Full	GLL190	418

- Although the Taguchi design represented the cooling time range between 344 s and 574 s for specific designs of nine parameters, the proposed correlation predicted the optimized cooling time of 334 s.
- Cooling performance of the ventilated disc affects its mechanical function in the form of thermal stress and residual thermal stresses. Thermomechanical analysis as well as investigation of the effects of the aforementioned parameters on the thermomechanical properties of the brake disc are the future works of this study.

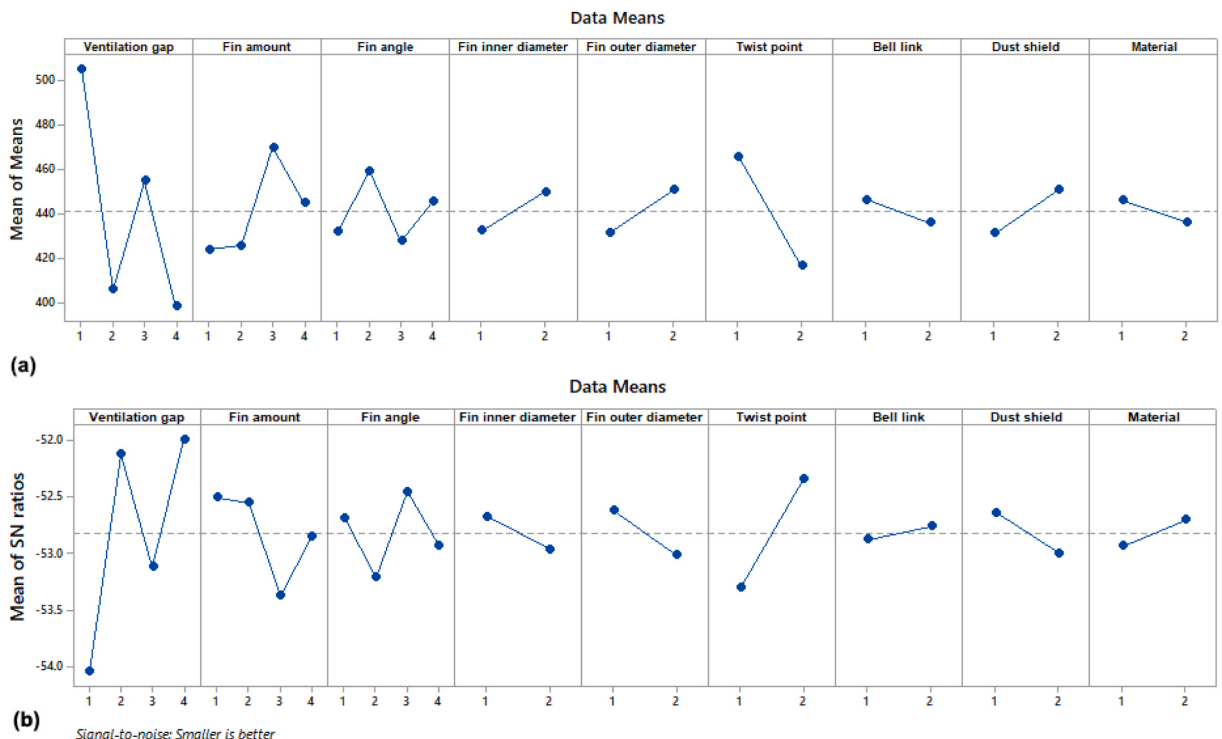


Fig. 12. Mean effect plots for (a) means, (b) S/N ratio.

**Table 5**  
Design parameters for Optimized ventilated brake disc.

Ventilation Gap (mm)	Fin Amount	Fin Angle (°)	Fin Inner diameter (mm)	Fin Outer diameter (mm)	Twist Point	Bell Link	Dust Shield	Material	Cooling Time (s)
14	30	37	5	9	266	2	1	1	336

## Author statement

RAHIM JAFARI: Methodology, Software, Formal analysis, Writing. RECEP AKYUZ: Conceptualization, Validation,

## Declaration of competing interest

The authors declare that they have no known competing financial interests or personal relationships that could have appeared to influence the work reported in this paper.

## References

- [1] T.K. Kao, J.W. Richmond, A. Douarre, Brake disc hot spotting and thermal judder: an experimental and finite element study, *Int. J. Veh. Des.* 23 (2000) 276–296, <https://doi.org/10.1504/ijvd.2000.001896>.
- [2] L. Augustins, F. Hild, R. Billardon, S. Boudevin, Experimental and numerical analysis of thermal striping in automotive brake discs, *Fatig. Fract. Eng. Mater. Struct.* 40 (2017) 267–276, <https://doi.org/10.1111/ffe.12495>.
- [3] J.E. Hunter, S.S. Cartier, D.J. Temple, R.C. Mason, Brake fluid vaporization as a contributing factor in motor vehicle collisions, *SAE Tech. Pap.* (1998), <https://doi.org/10.4271/980371>.
- [4] P. Grzes, W. Oliferuk, A. Adamowicz, K. Kochanowski, P. Wasilewski, A.A. Yevtushenko, The numerical-experimental scheme for the analysis of temperature field in a pad-disc braking system of a railway vehicle at single braking, *Int. Commun. Heat Mass Tran.* 75 (2016) 1–6, <https://doi.org/10.1016/j.icheatmasstransfer.2016.03.017>.
- [5] A.A. Alnagi, D.C. Barton, P.C. Brooks, Reduced scale thermal characterization of automotive disc brake, *Appl. Therm. Eng.* 75 (2015) 658–668, <https://doi.org/10.1016/j.applthermaleng.2014.10.001>.
- [6] A. Adamowicz, P. Grzes, Influence of convective cooling on a disc brake temperature distribution during repetitive braking, *Appl. Therm. Eng.* 31 (2011) 2177–2185, <https://doi.org/10.1016/j.applthermaleng.2011.05.016>.
- [7] P. Grzes, Maximum temperature of the disc during repeated braking applications, *Adv. Mech. Eng.* 11 (2019) 1–13, <https://doi.org/10.1177/1687814019837826>.
- [8] G. Le Gigan, T. Vernersson, R. Lundén, P. Skoglund, Disc brakes for heavy vehicles: an experimental study of temperatures and cracks, *Proc. Inst. Mech. Eng. - Part D J. Automob. Eng.* 229 (2015) 684–707, <https://doi.org/10.1177/0954407014550843>.
- [9] T. Schuetz, Cooling analysis of a passenger car disk brake, *SAE Tech. Pap.* 4970 (2009), <https://doi.org/10.4271/2009-01-3049>.

- [10] A. Coulibaly, N. Zioui, S. Bentouba, S. Kelouwani, M. Bourouis, Use of thermoelectric generators to harvest energy from motor vehicle brake discs, *Case Stud. Therm. Eng.* 28 (2021) 101379, <https://doi.org/10.1016/j.csite.2021.101379>.
- [11] C. Qian, Aerodynamic shape optimization using cfd parametric model with brake cooling application, *SAE Tech. Pap.* (2002), <https://doi.org/10.4271/2002-01-0599>.
- [12] G.P. Voller, M. Tirovic, R. Morris, P. Gibbens, Analysis of automotive disc brake cooling characteristics, *Proc. Inst. Mech. Eng. - Part D J. Automob. Eng.* 217 (2003) 657–666, <https://doi.org/10.1243/09544070360692050>.
- [13] R. Jafari, K.T. Erkiliç, O. Tekin, R. Akyüz, M. Gürer, Experimental and numerical study of turbulent flow and thermal behavior of automotive brake disc under repetitive braking, *Proc. Inst. Mech. Eng. - Part D J. Automob. Eng.* (2021), <https://doi.org/10.1177/09544070211040349>.
- [14] E. Palmer, R. Mishra, J. Fieldhouse, A computational fluid dynamic analysis on the effect of front row pin geometry on the aerothermodynamic properties of a pin-vented brake disc, *Proc. Inst. Mech. Eng. - Part D J. Automob. Eng.* 222 (2008) 1231–1245, <https://doi.org/10.1243/09544070JAU0755>.
- [15] E. Palmer, R. Mishra, J. Fieldhouse, An optimization study of a multiple-row pin-vented brake disc to promote brake cooling using computational fluid dynamics, *Proc. Inst. Mech. Eng. - Part D J. Automob. Eng.* 223 (2009) 865–875, <https://doi.org/10.1243/09544070JAU01053>.
- [16] P. Hwang, X. Wu, Y. Jeon, Repeated brake temperature analysis of ventilated brake disc on the downhill road, *SAE Tech. Pap.* (2008), <https://doi.org/10.4271/2008-01-2571>.
- [17] N.R. Stojanović, J.D. Gli, O.I. Abdullah, I. Ij, Pressure Influence on Heating of, (n.d.).
- [18] C.H. Galindo-Lopez, M. Tirovic, Understanding and improving the convective cooling of brake discs with radial vanes, *Proc. Inst. Mech. Eng. - Part D J. Automob. Eng.* 222 (2008) 1211–1229, <https://doi.org/10.1243/09544070JAUTO594>.
- [19] D.V.M. Pevec, I. Potrc, G. Bombek, Prediction of the cooling factors of a vehicle brake disc and its influence on the results of a thermal numerical simulation, *Int. J. Automot. Technol.* 13 (2012) 725–733.
- [20] A. Modanloo, M.R. Talaei, Analytical thermal analysis of advanced disk brake in high speed vehicles, *Mech. Adv. Mater. Struct.* 27 (2020) 209–217, <https://doi.org/10.1080/15376494.2018.1472340>.
- [21] H.B. Yan, T. Mew, M.G. Lee, K.J. Kang, T.J. Lu, F.W. Kienhöfer, T. Kim, Thermofluidic characteristics of a porous ventilated brake disk, *J. Heat Tran.* 137 (2015), <https://doi.org/10.1115/1.4028864>.
- [22] A. Kumar, R. Pandey, R. Kumar, N. Kumar, T.R. Kiran, Materials Today : proceedings Thermal analysis on car brake rotor using cast iron material with different geometries, *Mater. Today Proc.* 47 (2021) 7019–7024, <https://doi.org/10.1016/j.matpr.2021.05.299>.
- [23] A. Afzal, M.A. Mujeebu, Impact of curved vents , holes and slots on thermo-mechanical behavior of automobile disc brake, *FEM Simulation and Validation* 6 (2020) 21–39.
- [24] H.B. Yan, S.S. Feng, X.H. Yang, T.J. Lu, Role of cross-drilled holes in enhanced cooling of ventilated brake discs, *Appl. Therm. Eng.* 91 (2015) 318–333, <https://doi.org/10.1016/j.applthermaleng.2015.08.042>.
- [25] H. Yan, S. Feng, T. Lu, G. Xie, Experimental and numerical study of turbulent flow and enhanced heat transfer by cross-drilled holes in a pin-finned brake disc, *Int. J. Therm. Sci.* 118 (2017) 355–366, <https://doi.org/10.1016/j.ijthermalsci.2017.04.024>.
- [26] A. Vdovin, M. Gustafsson, S. Sebben, A coupled approach for vehicle brake cooling performance simulations, *Int. J. Therm. Sci.* 132 (2018) 257–266, <https://doi.org/10.1016/j.ijthermalsci.2018.05.016>.
- [27] L. Qiu, H.S. Qi, A. Wood, Two-dimensional finite element analysis investigation of the heat partition ratio of a friction brake, *Proc. Inst. Mech. Eng. Part J J. Eng. Tribol.* 232 (2018) 1489–1501, <https://doi.org/10.1177/1350650118757245>.
- [28] Q. Jian, L. Wang, Y. Shui, Thermal analysis of ventilated brake disc based on heat transfer enhancement of heat pipe, *Int. J. Therm. Sci.* 155 (2020) 106356, <https://doi.org/10.1016/j.ijthermalsci.2020.106356>.
- [29] H. Hong, G. Kim, H. Lee, J. Kim, D. Lee, M. Kim, M. Suh, J. Lee, Optimal location of brake pad for reduction of temperature deviation on brake disc during high-energy braking, *J. Mech. Sci. Technol.* 35 (2021) 1109–1120, <https://doi.org/10.1007/s12206-021-0224-x>.
- [30] H. Yan, W.T. Wu, S. Feng, G. Xie, Role of vane configuration on the heat dissipation performance of ventilated brake discs, *Appl. Therm. Eng.* 136 (2018) 118–130, <https://doi.org/10.1016/j.applthermaleng.2018.03.002>.
- [31] S. C., Y.W.G. Taguchi, *Taguchi's Quality Engineering Handbook*, John Wiley & Sons, Inc., New Jersey, 2004.
- [32] D.A. Johnson, B.A. Sperandei, R. Gilbert, Analysis of the flow through a vented automotive brake rotor, *J. Fluids Eng. Trans. ASME.* 125 (2003) 979–986, <https://doi.org/10.1115/1.1624426>.